Case Studies in Nondestructive Testing and Evaluation 4 (2015) 1–7

Contents lists available at ScienceDirect

Case Studies in Nondestructive Testing and Evaluation

www.elsevier.com/locate/csndt

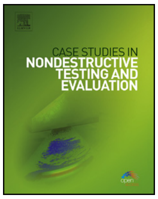

Application of microCT to the non-destructive testing of an additive manufactured titanium component

Anton du Plessis [a,*], Stephan G. le Roux [a], Johan Els [b], Gerrie Booysen [b], Deborah C. Blaine [c]

[a] *CT Scanner Facility, Stellenbosch University, Stellenbosch, South Africa*
[b] *Centre for Rapid Prototyping and Manufacturing, Central University of Technology, Bloemfontein, South Africa*
[c] *Mechanical Engineering, Stellenbosch University, Stellenbosch, South Africa*

ARTICLE INFO

Article history:
Available online 9 September 2015

ABSTRACT

In this paper the application of X-ray microCT to the non-destructive testing of an additive manufactured titanium alloy component of complex geometry is demonstrated. Additive manufacturing of metal components is fast growing and shows great promise, yet these parts may contain defects which affect mechanical properties of the components. In this work a layered form of defect is found by microCT, which would have been very difficult or impossible to detect by other non-destructive testing methods due to the object complexity, defect size and shape and because the pores are entirely contained inside the object and not connected to the surface. Additionally, this test part was subjected to hot isostatic pressing (HIPPING) and subsequently scanned. Comparing before and after scans by alignment of the volumes allows visualization and quantification of the pore size changes. The application of X-ray microCT to additive manufacturing is thus demonstrated in this example to be an ideal combination, especially for process improvements and for high value components.

1. Introduction

Additive Manufacturing (AM) has made significant progress in recent years, allowing complex parts to be manufactured layer by layer even in metals, with excellent material properties [1]. X-ray micro computed tomography (microCT) is a non-destructive testing method which has in recent years changed from a qualitative imaging to a quantitative measurement method in various applications, and especially in materials sciences [2,3]. MicroCT has been used successfully to measure the physical density of objects, using a calibration set of known samples of the same material as shown in [4] and quantitative and simple porosity analysis is possible providing information on pore sizes, shapes and more [5].

MicroCT has been applied to AM parts in various forms. Some preliminary results demonstrating the visualization of defects including porosity in AM components were reported in [6]. In another study, the porosity structures in parts built with improper settings were investigated [7]. In this work, the average porosity ranged from 0.1–0.5%, and large pores were observed which followed the build direction and may be attributed to the electron beam raster and overlap pattern. This was followed by more recent reports of the porosity distribution as a function of build strategy for electron beam

---

[*] Corresponding author. Tel.: +27 21 808 9389.
E-mail address: anton2@sun.ac.za (A. du Plessis).

http://dx.doi.org/10.1016/j.csndt.2015.09.001

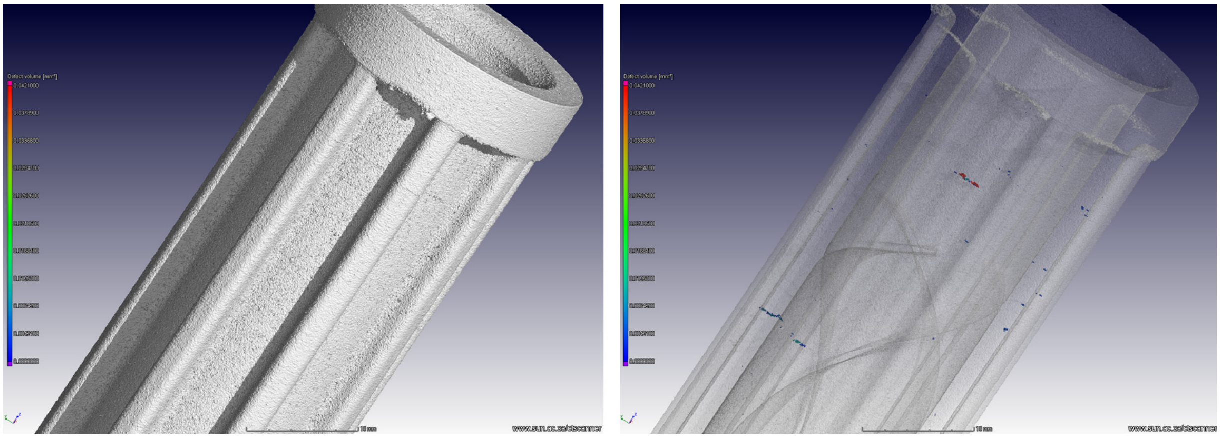

Fig. 1. A 3D view of the sample showing the surface (left) and the defects (right).

melted samples with average porosity $< 0.2\%$ [8]. In another study, similar porosity images from microCT were reported at levels above 0.2% average porosity [9,10]. Very recent work reports similar images and may indicate that the porosity structure depends on the build direction [11]. Other applications of the use of microCT to characterize AM parts include the comparison of the part to its design model [12] and the characterization of surface roughness of such parts [13]. In the present work, the aim is to demonstrate a specific type of defect present at very low average porosity levels below 0.01%, and which does not follow the build direction as in some other reported examples. We also demonstrate how this porosity structure changes after Hot Isostatic Pressing (HIP) treatment of the same sample.

2. Method

A geometrically complex Ti6Al4V component was manufactured as a test object on an EOS M270 (titanium version). This sample is approximately 30 mm in diameter and 60 mm high, with the build direction in the long axis. During the DMLS process of manufacturing this component it was observed that support structures from neighboring parts came loose from the titanium substrate/base. These loose support structures made lines through the powder bed during the recoating phase. The build was interrupted on several layers but it was decided to continue with the process to see afterwards which defects can be detected by microCT.

This sample was subjected to X-ray micro computed tomography (microCT), before and after HIP treatment. The microCT scans were done at 48 μm resolution, such that the entire sample fits in a single scan volume. These "before" and "after" scans were scanned and processed under identical conditions to ensure direct comparison is possible. A higher resolution scan at 25 μm was done additionally after treatment, by scanning the object in 4 parts and stitching the volumes together automatically. MicroCT scans were done with a General Electric Phoenix V|Tome|X L240 system at 160 kV and 100 μA, 500 ms per image, with 2000 images in one full rotation. Reconstruction is done with system-supplied software including beam hardening correction. The "before" scan of this object was reported in a conference paper without detailed analysis [6]. Subsequent HIP treatment and scans of the "after" state where done approximately 1 year later. The scan settings were chosen identical to facilitate best comparison. Due to the potential for improved image contrast, an improved scan with better resolution was also done at 25 μm as mentioned above.

All analyses reported here were done with Volume Graphics VGStudioMax 2.2 including the defect analysis module. For direct comparison of two volume data sets, both were imported into the same project and alignment done manually by rotating and moving the one object relative to the other. This was done in a manual process to ensure best overlap of exterior and interior surfaces, followed by an offset in one axis to view them side by side. In this way an unchanged pore could be visualized in the before and after condition and other changes viewed directly.

HIP treatment was done at Bodycote in Belgium at a temperature and pressure of $920\,^\circ\mathrm{C} +/- 10\,^\circ\mathrm{C}$ and 1000 bar for a dwell time of 120 minutes under an Argon atmosphere.

3. Results and discussion

The defects are clearly layered or flattened in shape as seen in the 3D image in Fig. 1. In this image, the defects are colour-coded with the largest void in red and smallest in blue. Slice images in Fig. 2 show more clearly the largest void region from top and side views. Clearly, the defects are found in a layered or flattened structure, with the defects in the plane of the laser melting process. This type of defect can be explained by imperfect melting on specific layers as explained in the previous section. This type of defect is difficult to detect by other means such as traditional radiographic testing, due to its size and geometry and the complexity of the object. The average porosity was measured using the automated defect

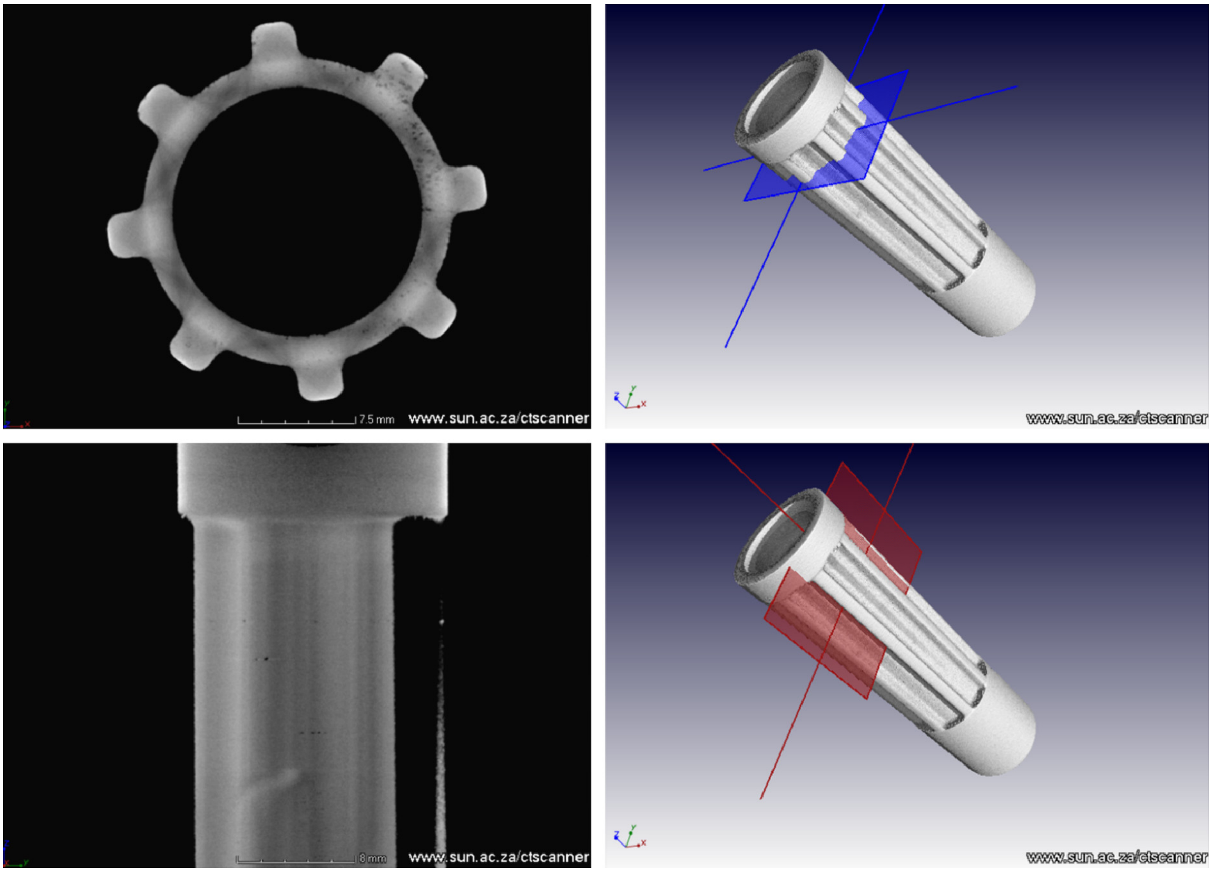

Fig. 2. Slice images from the top and side indicate the layered nature of the porosity.

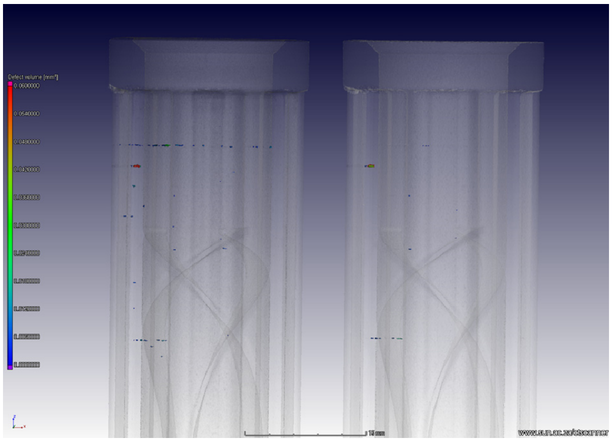

Fig. 3. Transparent 3D views before (left) and after (right) HIP treatment indicates qualitatively the lower average porosity after treatment.

analysis module as 0.005% before HIPping (excluding the base). This is extremely low, yet the structure of the porosity can have a definite impact on the part's mechanical properties.

Analysis of scans from before and after HIP treatment, using identical scan and analysis settings, indicates a reduced average porosity from 0.005% before HIP to 0.002% after HIP treatment. An automated defect analysis conducted on both samples shows this qualitatively in Fig. 3 in 3D.

For a more quantitative comparison, the before and after slice images can be compared side-by-side as shown in Fig. 4. For this type of analysis it is crucial for the accurate alignment, especially in the slice direction. This is done by comparing other physical features in slice images close to the images under consideration, to ensure direct comparison is possible.

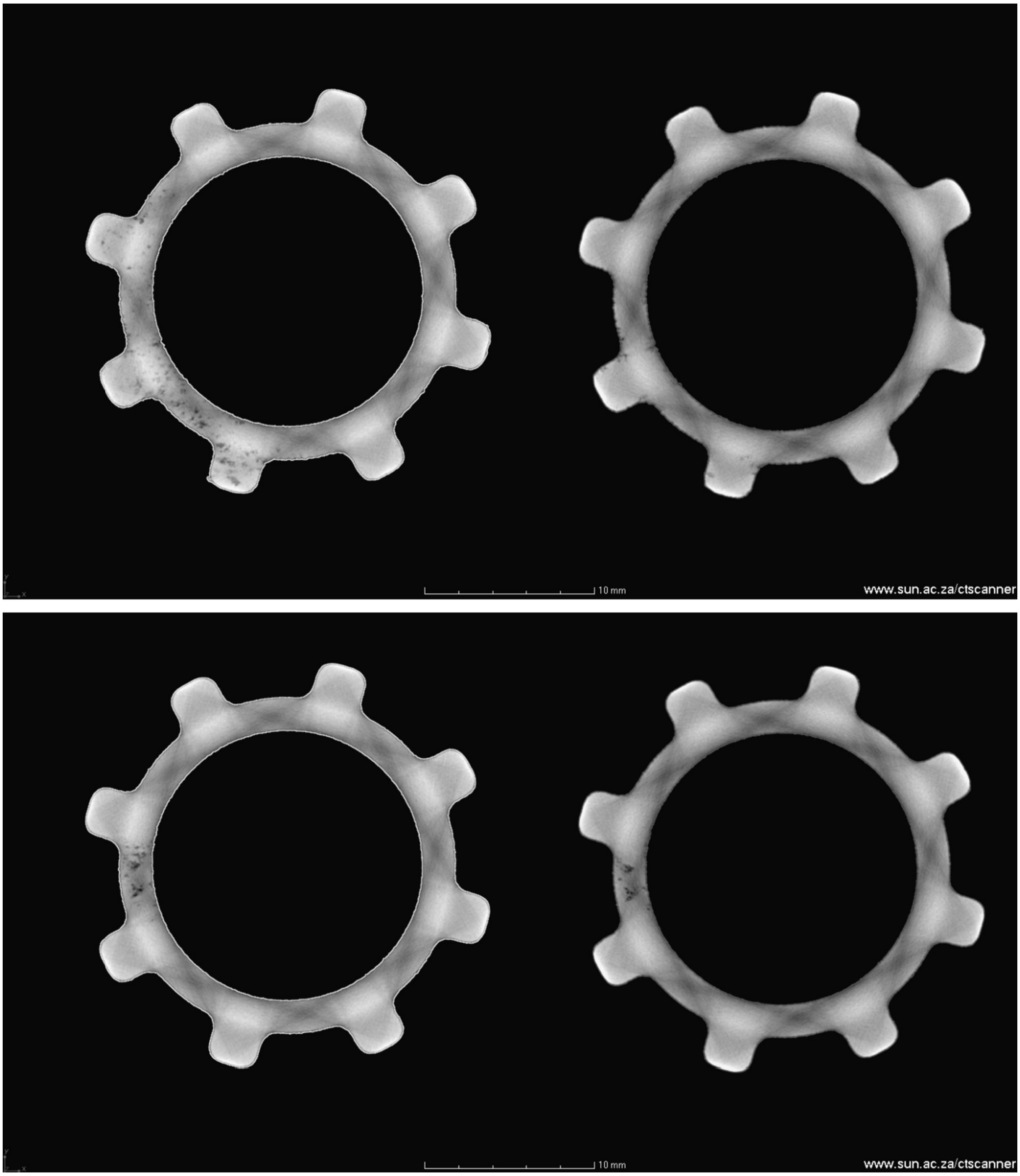

Fig. 4. Two examples of slice images side-by-side before and after HIP treatment, for which alignment is crucial. The first example shows porosity that is reduced while the second example shows one which remains unchanged.

In Fig. 4, two examples are shown at different heights along the sample. The first one is where the porosity reduces considerably due to HIPing, except for some pores near the edge of the object, most likely open pores connected to the surface. The second is an example where the pore structure remains effectively unchanged. This is unexpected and could be explained by the pore being connected to the surface via small porosity undetectable at this scan resolution.

An automated defect analysis can provide statistical information on the pore size distribution before and after HIP treatment. This is shown in Fig. 5, with counts scaled for direct comparison. The total number of pores reduced due to HIP treatment, as expected. The number of the smallest pores reduced considerably, while the largest pores are almost unchanged or only slightly reduced in size.

It is expected that HIP treatment closes pores very efficiently but the concept that the pores can remain but are smaller than the scan resolution is a topic of specific interest. A recent study in our group investigated the porosity of castings

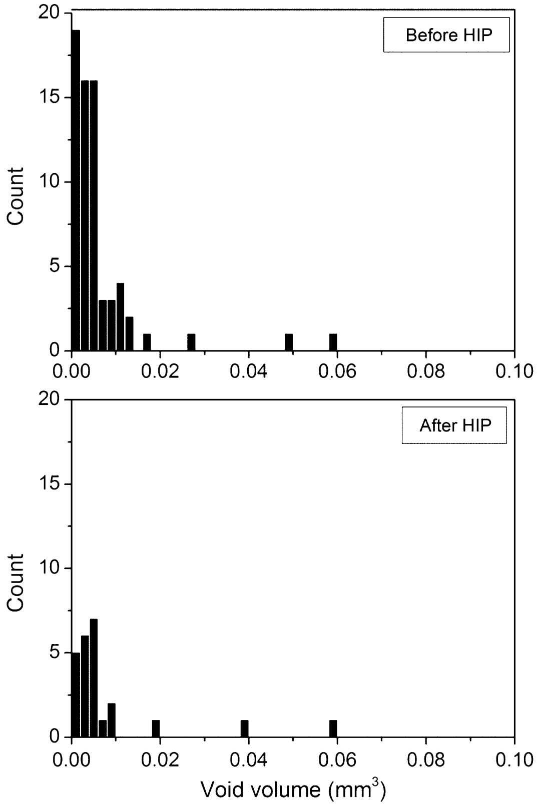

Fig. 5. Void size distribution before (top) and after (bottom) HIP treatment.

with large pore diameters up to 3 mm in size which entirely close up, even below the highest resolution limit of 6 µm (when the region of initial porosity is investigated as sectioned parts in high resolution scans) [14]. This work also included physical sectioning and no pores were found remaining except some small spherical voids which were close to the surface and unaffected by HIPping due to microcracks in the surface layer. Although this is a different type of sample, the closing of pores in this case is expected to be very good and when imaged at higher resolution after HIP treatment, no porosity was found in positions of closed-up pores. However some pores do remain unaffected here (especially the larger ones) and we can speculate that these larger pores are connected to the surface through microcracks thereby causing them to be unaffected by HIPping.

As additional proof of the porosity presence, a physical sectioning of the sample was done. The approximate location of the largest pore region from the CT scan data was used as a guide and physical sectioning and polishing was used producing optical micrographs as shown for two subsequent layers in Fig. 6 top and middle images. A higher resolution closeup view of the porosity region is shown in Fig. 6 as well, confirming the presence of pores indicated by CT scans. Additionally the shapes of the pores are seen to be very irregular.

4. Conclusion

It has been shown that a very specific type of layered defect can be formed in laser AM metal parts, most likely due to imperfect melting in specific layers. These defects are present in a part with as little as 0.005% porosity, but can still be a problem if localized in a thin walled section and is hence of importance in material studies and non-destructive testing of high-performance parts. X-ray microCT seems to be the ideal tool to characterize this type of defect due to the defect size and geometry, though X-ray microCT could also be used to indicate where to physically section a sample for further analysis. The HIP treatment efficiency could be assessed quantitatively and it can be concluded that the treatment is effective for pores smaller than 0.01 mm^3 but some larger layered defects can remain almost unchanged possibly due to connection to the surface, but it might be that the flat shape reduces the efficiency of HIP treatment. This visualization and characterization method holds promise for studies of improved material properties from additive manufacturing, and also generally for quality testing of HIPping and other material processing methods.

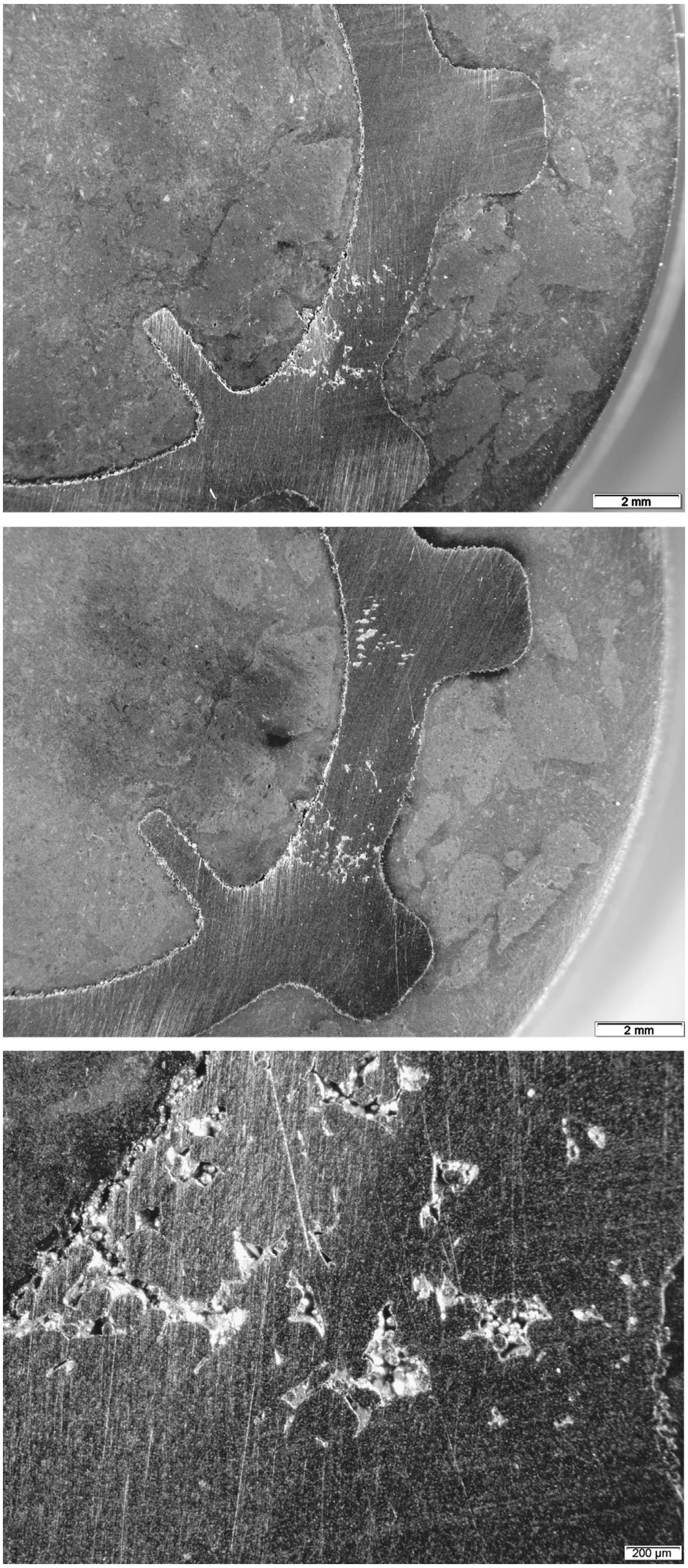

Fig. 6. Sectioning at the location indicated by the CT scans confirmed the presence of porosity in these micrograph images, where top and middle images show subsequent polished layers and the bottom image is a close-up view of the region of porosity in the middle image.

References

[1] Gu DD, Meiners W, Wissenbach K, Poprawe R. Laser additive manufacturing of metallic components: materials, processes and mechanisms. Int Mater Rev 2012;57(3):133–64.
[2] Maire E, Withers PJ. Quantitative X-ray tomography. Int Mater Rev 2014;59(1):1–43.
[3] Salvo L, Cloetens P, Maire E, Zabler S, Blandin JJ, Buffière JY, et al. X-ray micro-tomography an attractive characterisation technique in materials science. Nucl Instrum Methods Phys Res, Sect B, Beam Interact Mater Atoms 2003;200:273–86.
[4] du Plessis A, Meincken M, Seifert T. Quantitative determination of density and mass of polymeric materials using microfocus computed tomography. J Nondestruct Eval 2013;32(4).
[5] du Plessis A, Olawayu BJ, Boshoff WP, le Roux SG. Simple and fast porosity analysis of concrete using X-ray computed tomography. Mater Struct 2014:1–10. http://dx.doi.org/10.1617/s11527-014-0519-9.
[6] du Plessis A, Seifert T, Booysen G, Els J. Microfocus X-ray computed tomography (CT) analysis of laser sintered parts. S Afr J Ind Eng 2014;25(1):39–49.
[7] Léonard F, Tammas-Williams S, Prangnell PB, Todd I, Withers PJ. Assessment by X-ray CT of the effects of geometry and build direction on defects in titanium ALM parts. http://www.ndt.net/article/ctc2012/papers/91.pdf.
[8] Tammas-Williams S, Zhaoa H, Léonard F, Derguti F, Todd I, Prangnell PB. XCT analysis of the influence of melt strategies on defect population in Ti–6Al–4V components manufactured by selective electron beam melting. Mater Charact 2015;102:47–61.
[9] Vandenbroucke B, Kruth J-P. Selective laser melting of biocompatible metals for rapid manufacturing of medical parts. Rapid Prototyping J 2007;13(4):196–203.
[10] Kruth J-P, Levy G, Klocke F, Childs THC. Consolidation phenomena in laser and powder-bed based layered manufacturing. CIRP Ann 2007;56(2).
[11] Ziółkowski G, Chlebus E, Szymczyk P, Kurzac J. Application of X-ray CT method for discontinuity and porosity detection in 316L stainless steel parts produced with SLM technology. Arch Civ Mech Eng 2014;14(4):608–14.
[12] Van Bael S, Kerckhofs G, Moesen M, Pyka G, Schrooten J, Kruth JP. Micro-CT-based improvement of geometrical and mechanical controllability of selective laser melted Ti6Al4V porous structures. Mater Sci Eng A 2011;528:7423–31.
[13] Pyka G, Kerckhofs G, Papantoniou I, Speirs M, Schrooten J, Wevers M. Surface roughness and morphology customization of additive manufactured open porous Ti6Al4V structures. Materials 2013;6:4737–57.
[14] du Plessis A, Rossouw P. Investigation of porosity changes in cast Ti6Al4V rods after hot isostatic pressing. J Mater Eng Perform June 2015:21–6.